Symbolic-Numeric Solution of Boundary-Value Problems for the Schrödinger Equation Using the Finite Element Method: Scattering Problem and Resonance States

A.A. Gusev[1], L. Le Hai[1,2], O. Chuluunbaatar[1,3], V. Ulziibayar[4], S.I. Vinitsky[1], V.L. Derbov[5], A. Góźdź[6], and V.A. Rostovtsev[1]

[1] Joint Institute for Nuclear Research, Dubna, Russia
gooseff@jinr.ru
[2] Belgorod State University, Belgorod, Russia
[3] National University of Mongolia, UlaanBaatar, Mongolia
[4] Mongolian University of Science and Technology, UlaanBaatar, Mongolia
[5] Saratov State University, Saratov, Russia
[6] Institute of Physics, Maria Curie-Skłodowska University, Lublin, Poland

Abstract. We present new symbolic-numeric algorithms for solving the Schrödinger equation describing the scattering problem and resonance states. The boundary-value problems are formulated and discretized using the finite element method with interpolating Hermite polynomials, which provide the required continuity of the derivatives of the approximated solutions. The efficiency of the algorithms and programs implemented in the Maple computer algebra system is demonstrated by analysing the scattering problems and resonance states for the Schrödinger equation with continuous (piecewise continuous) real (complex) potentials like single (double) barrier (well).

1 Introduction

High-accuracy efficient algorithms and programs for solving boundary-value problems are presently indispensable for studying important mathematical models, describing wave propagation in smoothly irregular waveguides, tunnelling and channelling of compound quantum systems through multidimensional potential barriers, photoionization, photoabsorption, and transport in atomic, molecular, and quantum-dimensional semiconductor systems [1–15].

For this class of problems not only the solution itself, but also its first derivative must be continuous, which is of particular importance in the case of quantum-dimensional semiconductor systems and smoothly irregular waveguides, described by partial differential equations with piecewise-continuous coefficient functions [2, 16–18]. As shown by the example of solving an eigenvalue problem for the Schrödinger equation [19], the required continuity of the derivatives can be efficiently implemented in the approximating numerical solution on a finite-element grid using the Hermite interpolating elements [17, 20]. The reduction of the initial

V.P. Gerdt et al. (Eds.): CASC 2015, LNCS 9301, pp. 182–197, 2015.
DOI: 10.1007/978-3-319-24021-3_14

boundary-value problems to the corresponding algebraic problems is a cumbersome problem of the Finite Element Method using high-order approximation. The generation of the local functions using the high-order Hermite interpolation polynomials and the elements of mass and stiffness matrices is performed in the analytic form using the algorithm elaborated by the authors and implemented in CAS Maple. Using CAS Maple is a key point of the approach. Now it is possible to work with multiprocessor computers that implement parallel computations of algebraic problem with high-dimension matrices using the LinearAlgebra package of CAS Maple. Moreover, in our previous paper [19] we also used the symbolic algorithm to generate Fortran routines that allow the solution of the generalized algebraic eigenvalue problem with high-dimension matrices for real-valued potentials. Further development of this approach for solving the scattering problem and calculating the resonance metastable states for real-valued and complex potentials is an important problem that constitutes the goal of the present paper.

In this paper we present a new approach to the study of the resonance scattering problem and the metastable states for both continuous and piecewise continuous real-valued and complex potentials. The discretization of the corresponding boundary-value problem reformulated in terms of symmetric quadratic functionals is implemented using the Hermite interpolation polynomials which provide the required continuity of the derivatives of the approximated solutions. The continuity of the approximate solutions derivatives is the key point in the problems of quantum mechanics, waveguide theory, etc. For the scattering problem with the fixed real energy value $E{=}\Re E$, $\Re E{>}0$ we formulate the boundary-value problem for the Schrödinger equation in the finite interval $|z|{\le}|z^{\max}|$ with the conditions of the third kind at the boundary points of the interval and construct the appropriate variational functional. The asymptotic solutions of the scattering problem at $|z^{\max}| \le |z| < \infty$ comprise the incident wave and the unknown amplitudes of transmitted $T(E)$ and reflected $R(E)$ waves, which are calculated together with the desired numerical solution in the finite interval and its logarithmic derivatives at the boundary points of the interval. To calculate the resonance state with the unknown complex eigenvalue of energy $E_r{=}\Re E_r{+}\imath\Im E_r$, $\Re E_r{>}0$, $\Im E{<}0$ we formulate the boundary-value problem for the Schrödinger equation in the finite interval with the conditions of the third kind at the boundary points of the interval and construct the appropriate variational functional. In contrast to the scattering problem, in the asymptotic solutions of this problem the amplitude of the incident waves is zero, i.e., only the outgoing waves are present, $\exp(\imath\sqrt{E_r}|z|)$, that meet the radiation condition [23] and are considered within the sufficiently large but finite interval $|z|{\le}|z^{\max}|$.

The constructed stiffness and mass matrices for the variational functionals, comprising the boundary conditions of the first, second, or third kind, are used to formulate the generalized algebraic eigenvalue problem. To calculate the resonance states with unknown complex energy eigenvalues E_r we use the Newton iteration scheme, in which the initial approximation is chosen as the solution of the scattering problem with the boundary conditions of the third kind and the real values of energy $E{=}\Re E{>}0$, close to the resonance ones, $E_r{=}\Re E_r{+}\imath\Im E_r$, and corresponding to the maximal value of the transmission coefficient $|T(E)|^2$.

We also used the appropriate solutions of the eigenvalue problem with the boundary conditions of the first or the second kind.

The efficiency (the order of approximation with respect to the finite element grid step) and the capability of time saving (the execution time for the Maple algorithms for banded matrices with the dimension up to 300) is demonstrated by the test calculations of scattering and resonance states for the Schrödinger equation with continuous (piecewise continuous) real (complex) barrier (double barrier) or well (double well) potential functions.

The paper is organized as follows. In Section 2 the formulation of the boundary-value problems with the boundary conditions of the first, second, and third kind is presented, as well as the appropriate variational functionals. Sections 3 presents the finite-element scheme with the Hermite interpolating polynomials and describes the algorithm of reducing the boundary-value problems to the algebraic ones. Section 4 is devoted to test calculations that demonstrate the efficiency and time-saving capability of the proposed computational schemes, implemented as a Maple program. In the Conclusion we discuss the results and the possible applications of the proposed computational schemes and computer programs.

2 Formulation of Boundary-Value Problems

Consider the second-order differential equation with respect to the unknown function $\Phi(z)$ in the interval $z \in \Omega_z = (z^{\min}, z^{\max})$ [19]

$$(D-2E)\,\Phi(z) = 0, \quad D = -\frac{1}{f_1(z)}\frac{\partial}{\partial z} f_2(z) \frac{\partial}{\partial z} + V(z). \tag{1}$$

The coefficient functions $f_1(z) > 0$, $f_2(z) > 0$ and the real or complex potential function $V(z)$ are assumed to be continuous and to possess derivatives up to the order $\kappa^{\max}-1 \geq 1$ in the domain $z \in \bar{\Omega}_z = [z^{\min}, z^{\max}]$. Alternative assumptions for piecewise continuous functions will be also considered below.

Depending on the physical problem, the desired solution is to obey the appropriate boundary conditions at the end points $z^{\min}$ and $z^{\max}$ of the interval $\bar{\Omega}_z$:

$$\text{(I)}: \quad \Phi_m(z^t) = 0, \quad t = \min \text{ and/or } \max, \tag{2}$$

$$\text{(II)}: \quad d\Phi_m(z)/dz\big|_{z=z^t} = 0, \quad t = \min \text{ and/or } \max, \tag{3}$$

$$\text{(III)}: \quad d\Phi_m(z)/dz\big|_{z=z^t} = \mathcal{R}(z^t)\Phi_m(z^t), \quad t = \min \text{ and/or } \max. \tag{4}$$

The solution of the boundary-value problem can be reduced to the determination of the stationary point (or minimal value) of the variational functional [21]

$$\Xi(\Phi, E, z^{\min}, z^{\max}) \equiv \int_{z^{\min}}^{z^{\max}} \Phi(z)\,(D-2E)\,\Phi(z) f_1(z) dz = \Pi(\Phi, E, z^{\min}, z^{\max}) + C,$$
$$C = -f_2(z^{\max})\Phi(z^{\max})\mathcal{R}(z^{\max})\Phi(z^{\max}) + f_2(z^{\min})\Phi(z^{\min})\mathcal{R}(z^{\min})\Phi(z^{\min}), \tag{5}$$

where $\Pi(\Phi, E, z^{\min}, z^{\max})$ is the symmetric functional

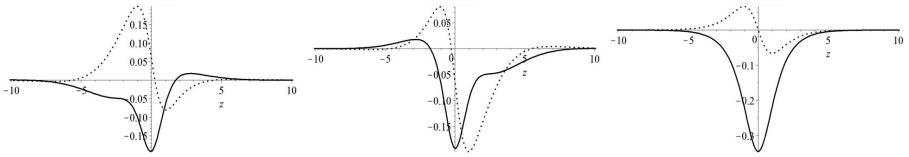

Fig. 1. Real (solid line) and imaginary (dotted line) parts of the eigenfunctions $\Phi_1^+(z)$, $\Phi_1^-(z)$ and $\Phi_1(z)$ with eigenvalues $E_1^{\pm}$ and E_1, respectively, given in Table 1.

$$\Pi(\Phi, E, z^{\min}, z^{\max}) = \int_{z^{\min}}^{z^{\max}} \big[f_2(z)d\Phi(z)/dzd\Phi(z)/dz + f_1(z)\Phi(z)V(z)\Phi(z) - f_1(z)2E\Phi(z)\Phi(z)\big]dz. \tag{6}$$

Problem 1. For bound states the eigenfunctions are considered that obey the boundary conditions of the second kind (3) or the first kind (2) for $\mathcal{R}(z) = 0$ or $\mathcal{R}(z) \to \infty$ in the functional (5), (6), respectively.

In the case (a) of the complex potential and complex eigenvalues $E_m = \Re E_m + \imath \Im E_m$ the eigenfunctions $\Phi_m(z)$ obey the normalization and orthogonality conditions

$$\langle \Phi_m | \Phi_{m'} \rangle = \int_{z^{\min}}^{z^{\max}} \Phi_m(z)\Phi_{m'}(z)f_1(z)dz = \delta_{mm'}. \tag{7}$$

In the case (b) of the real eigenvalues E_m, i.e., $E_m = E_m^*$, $\Im E = 0$, the left-hand function $\Phi_m(z)$ in the scalar product (7) and the functional (5), (6) is replaced with the complex conjugate function $\Phi_m^*(z)$, corresponding to the same eigenvalue $E_m^* = E_m$.

Problem 2. For solving the scattering problem with fixed real eigenvalues E the eigenfunctions $\Phi(E, z)$ are to satisfy the boundary conditions of the third kind (4). The asymptotic solutions of the scattering problem at $|z^{\max}| \le |z| < \infty$ comprise the incident wave and the unknown amplitudes of transmitted $T(E)$ and reflected $R(E)$ waves, which are calculated together with the desired numerical solution in the finite interval and its logarithmic derivatives $\mathcal{R}(z^t)$ at the boundary points of the interval. The unknown eigenvalues $\mathcal{R}(z^{\min})$ (or $\mathcal{R}(z^{\max})$) are determined by solving the problem (19) with the boundary conditions (4) taken into account in a way similar to [9]. The parameter $\mathcal{R}(z^t)$, $t = \max$ (or $t = \min$), in the functional (5), (6) is determined from the asymptotic boundary conditions, $\mathcal{R}(z^t) = \left.\frac{d\Phi_{as}(E,z)}{dz}\right|_{z=z^t} \frac{1}{\Phi_{as}(E,z^t)}$, where the asymptotic solutions $\Phi_{as}(E, z)$ are δ-function normalized.

In the case (a) of the complex potential the eigenfunctions $\Phi(E,z)$ obey the normalization and orthogonality conditions

$$\langle\Phi(E)|\Phi(E')\rangle = \int_{z^{\min}}^{z^{\max}} \Phi(E,z)\Phi(E',z)f_1(z)dz + C(E,E') = 2\pi\delta(E-E'), \quad (8)$$

$$C(E,E') = \int_{-\infty}^{z^{\min}} \Phi_{as}(E,z)\Phi_{as}(E',z)f_1(z)dz + \int_{z^{\max}}^{+\infty} \Phi_{as}(E,z)\Phi_{as}(E',z)f_1(z)dz.$$

In the case (b) of the real potential the left-hand function $\Phi(E,z)$ in the scalar product (8) and in the functional (5), (6) is replaced with the complex conjugate eigenfunction $\Phi^*(E,z)$. The detailed consideration of the asymptotic functions $\Phi_{as}(E,z)$ will be presented below.

Problem 3. For metastable states the solution satisfies the boundary conditions of the third kind (4), where the parameter $\mathcal{R}(z^t)$ depends upon the complex energy value $E = \Re E + \imath\Im E$ in the lower semiplane: $\mathcal{R}(z^{\min}) = -\sqrt{-2E}$, $\mathcal{R}(z^{\max}) = \sqrt{-2E}$, with $\Re E > 0$ and $\Im E < 0$. In this case for the real (b) and complex (a) potentials (provided that the real and imaginary parts of the latter are specifically chosen, see [13]) the solution satisfies the normalization condition

$$(\Phi_m|\Phi_m) = 2\sqrt{-2E_m}\left(\int_{z^{\min}}^{z^{\max}} \Phi_m(z)\Phi_m(z)f_1(z)dz - 1\right) + C_{mm} = 0, \quad (9)$$

$$C_{mm} = -f_2(z^{\max})\Phi_m(z^{\max})\Phi_m(z^{\max}) + f_2(z^{\min})\Phi_m(z^{\min})\Phi_m(z^{\min}),$$

and the orthogonality condition

$$(\Phi_m|\Phi_{m'}) = (\sqrt{-2E_m} + \sqrt{-2E_{m'}}) \int_{z^{\min}}^{z^{\max}} \Phi_m(z)\Phi_{m'}(z)f_1(z)dz + C_{mm'} = 0, \quad (10)$$

$$C_{mm'} = -f_2(z^{\max})\Phi_m(z^{\max})\Phi_{m'}(z^{\max}) + f_2(z^{\min})\Phi_m(z^{\min})\Phi_{m'}(z^{\min}),$$

that follows from calculating the difference of the functionals (5) with the eigenvalues E_m, $E_{m'}$ and the corresponding eigenfunctions $\Phi_m(z)$, $\Phi_{m'}(z)$ substituted into them and with $\imath p_m = \imath\sqrt{2E_m}$ and $\imath p_{m'} = \imath\sqrt{2E_{m'}}$ substituted into the parameter $\mathcal{R}(z^{\max})$ and with inverse sign into the parameter $\mathcal{R}(z^{\min})$, respectively. Similar orthogonality condition for real potentials was derived earlier using the Green function of the semiaxis [22].

2.1 Scattering Problem: The Physical Asymptotic Solutions in Longitudinal Coordinates and the Scattering Matrix

The solutions of the scattering problem with the fixed energy value $E > 0$ normalized by the condition (8) on the axis $z \in (-\infty, +\infty)$ possess the "incident wave + outgoing waves" asymptotic form

$$\boldsymbol{\Phi}_v(z \to \pm\infty) = \begin{cases} \begin{cases} X^{(+)}(z)T_v, & z > 0, \\ X^{(+)}(z) + X^{(-)}(z)R_v, & z < 0, \end{cases} & v = \rightarrow, \\ \begin{cases} X^{(-)}(z) + X^{(+)}(z)R_v, & z > 0, \\ X^{(-)}(z)T_v, & z < 0, \end{cases} & v = \leftarrow, \end{cases} \quad (11)$$

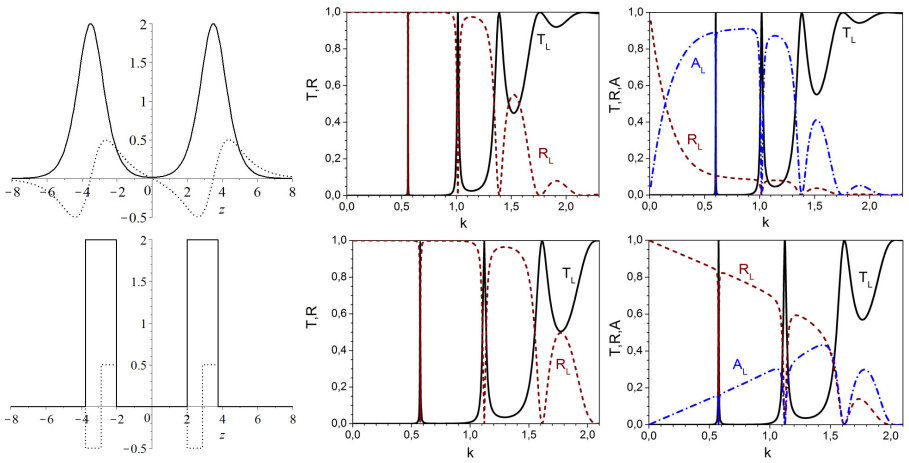

Fig. 2. The system of two complex Scarf potentials with $V_1 = 2$, $V_2 = 1$ separated by the distance $d = 7/2$, and the system of two complex rectangular potential barriers. The solid line shows the real part and the dotted line shows the imaginary part (left-hand panel). The coefficients of transmission $T_L = |T_{\rightarrow}|^2$ (solid line), reflection $R_L = |R_{\rightarrow}|^2$ (dotted line), and absorption A_L (dash-dotted line) versus the wave number $k = \sqrt{2E}$ for the systems of two purely real potentials (center panel) and complex potentials (right-hand panel).

where T_v and R_v are the transmission and reflection amplitudes, v is the initial direction of the particle motion along the z axis. For example, for $f_1(z) = f_2(z) = 1$ and rapidly decreasing $V(z \to \pm\infty) \to 0$ the asymptotic solutions $X^{(\pm)}(z) \equiv X^{(\pm)}(z, E)$ have the form

$$X^{(\pm)}(z) \to (p)^{-1/2} \exp(\pm \imath p z), p = \sqrt{2E} \tag{12}$$

with the normalization condition

$$\int_{-\infty}^{\infty} (X^{(\pm)}(z, E'))^* X^{(\pm)}(z, E) dz = 2\pi\delta(E' - E). \tag{13}$$

Generally, the functions $X^{(\pm)}(z)$ satisfy the conditions with the Wronskian

$$\begin{aligned} &\mathrm{Wr}(X^{(\mp)}(z), X^{(\pm)}(z)) = \pm 2\imath, \quad \mathrm{Wr}(X^{(\pm)}(z), X^{(\pm)}(z)) = 0, \\ &\mathrm{Wr}(a(z), b(z)) = f_2(z)\,(a(z)db(z)/dz - da(z)/dz b(z))\,. \end{aligned} \tag{14}$$

For real-valued potentials the Wronskian is constant, which yields the following properties of the reflection and transmission amplitudes

$$T^*_{\rightarrow}T_{\rightarrow} + R^*_{\rightarrow}R_{\rightarrow} = T^*_{\leftarrow}T_{\leftarrow} + R^*_{\leftarrow}R_{\leftarrow} = 1, \quad T_{\rightarrow} = T_{\leftarrow}$$
$$T^*_{\rightarrow}R_{\leftarrow} + R^*_{\rightarrow}T_{\leftarrow} = R^*_{\leftarrow}T_{\rightarrow} + T^*_{\leftarrow}R_{\rightarrow} = 0, \tag{15}$$

as well as the symmetric and unitary properties of the scattering matrix

$$\mathbf{S} = \begin{pmatrix} R_{\rightarrow} & T_{\leftarrow} \\ T_{\rightarrow} & R_{\leftarrow} \end{pmatrix}, \qquad \mathbf{S}^{\dagger}\mathbf{S} = \mathbf{S}\mathbf{S}^{\dagger} = 1. \tag{16}$$

3 Generation of Algebraic Problems

First, the initial interval $[z^{\min}, z^{\max}]$ is divided into n' subintervals $\tilde{\Omega}_i = [z'_{i-1}, z'_i]$, each of them being divided into n_i finite elements of different length $h_i = (z'_i - z'_{i-1})/n_i$. As a result we arrive at the following partitioning of the domain into $n = n_1 + ... + n_i + ... + n_{n'} \geq n'$ finite elements

$$\Omega^p_{h_j(z)}[z^{\min}, z^{\max}] = \cup_{j=1}^{n}\Omega_j = \cup_{i=1}^{n'}\bar{\Omega}_i, \quad \bar{\Omega}_i = \cup_{j=n_1+...+n_{i-1}+1}^{n_1+...+n_{i-1}+n_i}\Omega_j, \tag{17}$$
$$\Omega_j = [z_j^{\min}, z_j^{\max} \equiv z_{j+1}^{\min}], \quad j = 0, ..., n,$$
$$z^{\max}_{j=i'+n_1+...+n_{i-1}} = (z'_{i-1}(n_i - i') + z'_i i')/n_i, \quad i' = 0, ..., n_i, \quad i = 1, ..., n'.$$

Each of the finite elements is then divided into p similar intervals, thus forming the finite-element grid $\Omega^p_{h_j(z)}[z^{\min}, z^{\max}] = \{z_0, z_1, ..., z_{np}\}$, where $z_{p(j-1)+r} = (z_j^{\min}(p-r) + z_j^{\max} r)/p$, $r = 0, ..., p$.

The solutions $\hat{\Phi}(z)$ are sought for in the form of a finite sum over the basis of local functions $N^g_\mu(z)$ at each nodal point $z = z_k$ of the grid $\Omega^p_{h_j(z)}[z^{\min}, z^{\max}]$:

$$\hat{\Phi}(z) = \sum_{\mu=0}^{L-1} \Phi^h_\mu N^g_\mu(z), \quad \hat{\Phi}(z_l) = \Phi^h_{l\kappa^{\max}}, \quad d^\kappa\hat{\Phi}(z)/dz^\kappa\big|_{z=z_l} = \Phi^h_{l\kappa^{\max}+\kappa} \tag{18}$$

where $L = (pn+1)\kappa^{\max}$ is the number of local functions and Φ^h_μ at $\mu = l\kappa^{\max} + \kappa$ are the nodal values of the κ-th derivatives of the function $\hat{\Phi}(z)$ (including the function $\hat{\Phi}(z)$ itself for $\kappa = 0$) at the points z_l.

The local functions $N^g_\mu(z) \equiv N^g_{l\kappa^{\max}+\kappa}(z)$ are piecewise polynomials of the given order $p' = \kappa^{\max}(p+1) - 1$, constructed in our previous paper [19]. Their derivative of the order κ at the node z_l equals one, and the derivative of the order $\kappa' \neq \kappa$ at this node equals zero, while the values of the function $N^g_\mu(z)$ with all its derivatives up to the order $(\kappa^{\max} - 1)$ equal zero at all other nodes $z_{l'} \neq z_l$ of the grid $\Omega^p_{h_j(z)}[z^{\min}, z^{\max}]$, i.e., $d^\kappa N^g_{l'\kappa^{\max}+\kappa'}/dz^\kappa\big|_{z=z_l} = \delta_{ll'}\delta_{\kappa\kappa'}$, $l = 0, \ldots, np$, $\kappa = 0, \ldots, \kappa^{\max} - 1$.

The substitution of the expansion (18) into the variational functional (5), (6) reduces the solution of the eigenvalue *problem 1 or 3* (1)–(4) with the normalization condition (7)) or (9), or the scattering *problem 2* (1)–(4) with the fixed energy E to the solution of the algebraic problem with respect to the desired set $\boldsymbol{\Phi}^h = \{\Phi^h_\mu\}_{\mu=0}^{L-1}$:

$$(\mathbf{A} - \mathbf{M}_{\max} + \mathbf{M}_{\min} - 2E\,\mathbf{B})\boldsymbol{\Phi}^h = 0. \tag{19}$$

Here $\mathbf{A}$ and $\mathbf{B}$ are the symmetric $L \times L$ stiffness and mass matrices, $L = \kappa^{\max}(np+1)$,

$$A_{\mu_1;\mu_2} = \int_{z^{\min}}^{z^{\max}} f_2(z)\frac{dN^g_{\mu_1}(z)}{dz}\frac{dN^g_{\mu_2}(z)}{dz}dz + \int_{z^{\min}}^{z^{\max}} f_1(z)dzN^g_{\mu_1}(z)V(z)N^g_{\mu_2}(z),$$

$$B_{l_1;l_2} = \int_{z^{\min}}^{z^{\max}} f_1(z)N^g_{\mu_1}(z)N^g_{\mu_2}(z)dz,$$

$\mathbf{M}_{\max}$ and $\mathbf{M}_{\min}$ are $L \times L$ the matrices with zero elements except $M_{11} = f_2(z^{\min})\,\mathcal{R}(z^{\min})$ and $M_{L+1-\kappa^{\max},\,L+1-\kappa^{\max}} = f_2(z^{\max})\,\mathcal{R}(z^{\max})$, respectively. The unknown eigenvalues $\mathcal{R}(z^{\min})$ or $\mathcal{R}(z^{\max})$ are determined by solving the problem (19) with the boundary conditions (4) taken into account in a way similar to that of Ref. [9].

The theoretical estimate for the $\mathbf{H^0}$ norm of the difference between the exact solution $\Phi_m(z) \in \mathcal{H}_2^2$ and the numerical one $\Phi^h_m(z) \in \mathbf{H}^{\kappa^{\max}}$ has the order of

$$|E^h_m - E_m| \le c_1\, h^{2p'}, \quad \left\|\Phi^h_m(z) - \Phi_m(z)\right\|_0 \le c_2 h^{p'+1}, \tag{20}$$

where $h = \max_{1<j<n} h_j$ is the maximal step of the grid [21].

Remark. To obtain the eigenvalue estimate of the order $2p'$ the integrals are to be calculated with the same order of accuracy $2p'$. If the integrals are calculated with the accuracy $p'+1$, then we get the estimate of the same order $p'+1$ both for eigenvalues and for eigenfunctions.

3.1 The Calculation Scheme for the Solution Matrix $\boldsymbol{\Phi^h} = \boldsymbol{\Phi^h_{\leftarrow}}$

In this case Eq. (19) can be written in the following form

$$(\mathbf{G} + \mathbf{M}_{\min})\begin{pmatrix}\boldsymbol{\Phi}^a_{\leftarrow}\\ \boldsymbol{\Phi}^b_{\leftarrow}\end{pmatrix} \equiv \begin{pmatrix}\mathbf{G}^{aa}_{\leftarrow} & \mathbf{G}^{ab}_{\leftarrow}\\ \mathbf{G}^{ba}_{\leftarrow} & \mathbf{G}^{bb}_{\leftarrow}\end{pmatrix}\begin{pmatrix}\boldsymbol{\Phi}^a_{\leftarrow}\\ \boldsymbol{\Phi}^b_{\leftarrow}\end{pmatrix} = \begin{pmatrix}\mathbf{0} & \mathbf{0}\\ \mathbf{0} & \mathbf{G}(z^{\max})\end{pmatrix}\begin{pmatrix}\boldsymbol{\Phi}^a_{\leftarrow}\\ \boldsymbol{\Phi}^b_{\leftarrow}\end{pmatrix}, \tag{21}$$

where $(\mathbf{M}_{\min})_{11} = M_{11} = f_2(z^{\min})\mathcal{R}(z^{\min})$, $\mathcal{R}(z^{\min}) = \imath\sqrt{2E}$, the solutions $\boldsymbol{\Phi}^a_{\leftarrow}$ and $\boldsymbol{\Phi}^b_{\leftarrow} \equiv \Phi_{\leftarrow}(z^{\max})$ are vectors with the dimension $(L-1)$ and 1, respectively.

Hence the explicit expressions follow

$$\boldsymbol{\Phi}^a_{\leftarrow} = -(\mathbf{G}^{aa}_{\leftarrow})^{-1}\mathbf{G}^{ab}_{\leftarrow}\boldsymbol{\Phi}^b_{\leftarrow}, \quad \mathbf{G}(z^{\max}) = \mathbf{G}^{bb}_{\leftarrow} - \mathbf{G}^{ba}_{\leftarrow}(\mathbf{G}^{aa}_{\leftarrow})^{-1}\mathbf{G}^{ab}_{\leftarrow}. \tag{22}$$

From Eqs. (21) and (22) the relation between $\boldsymbol{\Phi}^b_{\leftarrow}$ and its derivative follows

$$d\boldsymbol{\Phi}^b_{\leftarrow}/dz = \mathcal{R}(z^{\max})\boldsymbol{\Phi}^b_{\leftarrow}, \quad \mathcal{R}(z^{\max}) = \mathbf{G}(z^{\max}). \tag{23}$$

Note, that the matrix $\mathbf{G}(z^{\max})$ is defined as the inverse of the submatrix $\mathbf{G}^{aa}_{\leftarrow}$, the calculation of which requires significant computer resources. To solve Eq. (23) without inverting $\mathbf{G}^{aa}_{\leftarrow}$, let us consider the set of algebraic equations with respect to the vectors $\mathbf{F}^a_{\leftarrow}$ and $\mathbf{F}^b_{\leftarrow}$

$$\begin{pmatrix}\mathbf{G}^{aa}_{\leftarrow} & \mathbf{G}^{ab}_{\leftarrow}\\ \mathbf{G}^{ba}_{\leftarrow} & \mathbf{G}^{bb}_{\leftarrow}\end{pmatrix}\begin{pmatrix}\mathbf{F}^a_{\leftarrow}\\ \mathbf{F}^b_{\leftarrow}\end{pmatrix} = f_2(z^{\max})\begin{pmatrix}0\\ \mathbf{I}\end{pmatrix}. \tag{24}$$

Since the determinant of the matrix $\mathbf{G}+\mathbf{M}_{\min}$ is nonzero, the set of equations has the unique solution

$$\mathbf{F}^a_{\leftarrow}=-(\mathbf{G}^{aa}_{\leftarrow})^{-1}\mathbf{G}^{ab}_{\leftarrow}\mathbf{F}^b_{\leftarrow},\quad \mathbf{F}^b_{\leftarrow}=f_2(z^{\max})\left(\mathbf{G}^{bb}_{\leftarrow}-\mathbf{G}^{ba}_{\leftarrow}(\mathbf{G}^{aa}_{\leftarrow})^{-1}\mathbf{G}^{ab}_{\leftarrow}\right)^{-1}. \quad (25)$$

Then the expression for $\mathcal{R}(z^{\max})$ follows

$$\mathcal{R}(z^{\max})=\left(\mathbf{F}^b_{\leftarrow}\right)^{-1}. \quad (26)$$

From Eqs. (23) and (11) we get the equation for the reflection amplitude $R_{\leftarrow}$:

$$Y^{(+)}_{\leftarrow}(z^{\max})R_{\leftarrow}=-Y^{(-)}_{\leftarrow}(z^{\max}),\quad Y^{(\pm)}_{\leftarrow}(z)=dX^{(\pm)}(z)/dz-\mathcal{R}(z)X^{(\pm)}(z). \quad (27)$$

Having solved this equation, we find the reflection amplitude $R_{\leftarrow}$

$$R_{\leftarrow}=-(Y^{(+)}_{\leftarrow}(z^{\max}))^{-1}Y^{(-)}_{\leftarrow}(z^{\max}). \quad (28)$$

Then the desired solution $\boldsymbol{\Phi}^h_{\leftarrow}$ is calculated from Eqs. (11), (22), and (25)

$$\boldsymbol{\Phi}^b_{\leftarrow}=X^{(-)}(z^{\max})+X^{(+)}(z^{\max})R_{\leftarrow},\quad \boldsymbol{\Phi}^a_{\leftarrow}=F^a_{\leftarrow}\left(F^b_{\leftarrow}\right)^{-1}\boldsymbol{\Phi}^b_{\leftarrow}. \quad (29)$$

The transmission amplitude $T_{\leftarrow}$ is determined by solving the equation

$$X^{(-)}(z^{\min})T_{\leftarrow}=\boldsymbol{\Phi}^h_{\leftarrow}(z^{\min}),\quad T_{\leftarrow}=\left(X^{(-)}(z^{\min})\right)^{-1}\Phi^h_{\leftarrow}(z^{\min}).$$

3.2 The Calculation Scheme for the Solution Matrix $\boldsymbol{\Phi^h=\Phi^h_{\rightarrow}}$

In this case Eq. (19) can be written as follows:

$$(\mathbf{G}-\mathbf{M}_{\max})\begin{pmatrix}\boldsymbol{\Phi}^a_{\rightarrow}\\ \boldsymbol{\Phi}^b_{\rightarrow}\end{pmatrix}\equiv\begin{pmatrix}\mathbf{G}^{aa}_{\rightarrow}&\mathbf{G}^{ab}_{\rightarrow}\\ \mathbf{G}^{ba}_{\rightarrow}&\mathbf{G}^{bb}_{\rightarrow}\end{pmatrix}\begin{pmatrix}\boldsymbol{\Phi}^a_{\rightarrow}\\ \boldsymbol{\Phi}^b_{\rightarrow}\end{pmatrix}=\begin{pmatrix}-\mathbf{G}(z^{\min})&\mathbf{0}\\ \mathbf{0}&\mathbf{0}\end{pmatrix}\begin{pmatrix}\boldsymbol{\Phi}^a_{\rightarrow}\\ \boldsymbol{\Phi}^b_{\rightarrow}\end{pmatrix}, \quad (30)$$

where $(\mathbf{M}^p_{\max})_{LL}=M_{L+1-\kappa^{\max},L+1-\kappa^{\max}}=f_2(z^{\max})\mathcal{R}(z^{\max})$, $\mathcal{R}(z^{\max})=-\imath\sqrt{2E}$, the solutions $\boldsymbol{\Phi}^a_{\rightarrow}$ and $\boldsymbol{\Phi}^b_{\rightarrow}\equiv\Phi_{\rightarrow}(z_{\min})$ are vectors with the dimension 1 and $(L-1)$, respectively.

The desired matrix $\mathbf{G}(z^{\min})=\mathcal{R}(z^{\min})$ is expressed as

$$\mathcal{R}(z^{\min})=(\mathbf{F}^a_{\rightarrow})^{-1}, \quad (31)$$

and the desired solution $\boldsymbol{\Phi}^h_{\rightarrow}$ is calculated as

$$\boldsymbol{\Phi}^b_{\rightarrow}=\mathbf{F}^b_{\rightarrow}(\mathbf{F}^a_{\rightarrow})^{-1}\boldsymbol{\Phi}^a_{\rightarrow},\qquad \boldsymbol{\Phi}^a_{\rightarrow}=X^{(+)}(z^{\min})+X^{(-)}(z^{\min})R_{\rightarrow}. \quad (32)$$

Here $\boldsymbol{\Phi}^a_{\rightarrow}\equiv\boldsymbol{\Phi}_{\rightarrow}(z^{\min})$ and $\boldsymbol{\Phi}^b_{\rightarrow}$ are vectors with the dimension 1 and $(L-1)$. The column vectors $\mathbf{F}^a_{\rightarrow}$ and $\mathbf{F}^b_{\rightarrow}$ with the dimension 1 and $(L-1)$ are solutions of the sets of algebraic equations

$$(\mathbf{G}-\mathbf{M}_{\max})\begin{pmatrix}\mathbf{F}^a_{\rightarrow}\\ \mathbf{F}^b_{\rightarrow}\end{pmatrix}\equiv\begin{pmatrix}\mathbf{G}^{aa}_{\rightarrow}&\mathbf{G}^{ab}_{\rightarrow}\\ \mathbf{G}^{ba}_{\rightarrow}&\mathbf{G}^{bb}_{\rightarrow}\end{pmatrix}\begin{pmatrix}\mathbf{F}^a_{\rightarrow}\\ \mathbf{F}^b_{\rightarrow}\end{pmatrix}=-f_2(z^{\min})\begin{pmatrix}\mathbf{I}\\ 0\end{pmatrix}. \quad (33)$$

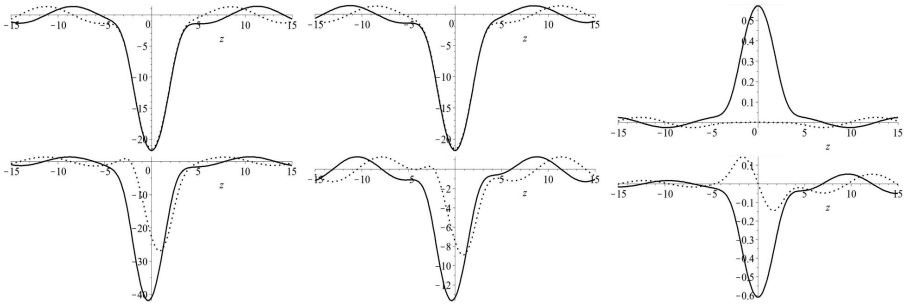

Fig. 3. Wave functions of the scattering problem for the first resonance value of energy $2E_1^{\max T}$, corresponding to the full transparency, i.e., the maximal transmission coefficient, for $\Phi_{\rightarrow}$ (left-hand panels) and $\Phi_{\leftarrow}$ (central panels); the functions of resonance metastable states with the energies $2E_1^{r}$ (right-hand panels), respectively, given in Table 3. The upper panels refer to the system of two real Scarf potentials with $V_1 = 2$, $V_2 = 0$, the lower panels refer to the system of two complex Scarf potentials with $V_1 = 2$, $V_2 = 1$. Solid and dotted lines show the real and imaginary parts of the wave functions, respectively.

Finally, we arrive at the following equations for the amplitudes of reflection $R_{\rightarrow}$ and transmission $T_{\rightarrow}$:

$$Y_{\rightarrow}^{(-)}(z^{\min})R_{\rightarrow} = -Y_{\rightarrow}^{(+)}(z^{\min}), \quad X^{(+)}(z_{\max})T_{\rightarrow} = \Phi_{\rightarrow}^{h}(z_{\max}), \tag{34}$$

$$Y_{\rightarrow}^{(\pm)}(z) = \frac{dX^{(\pm)}(z)}{dz} - \mathcal{R}(z)X^{(\pm)}(z). \tag{35}$$

The amplitudes of reflection $R_{\rightarrow}$ and transmission $T_{\rightarrow}$ take the form

$$R_{\rightarrow} = -\left(Y_{\rightarrow}^{(-)}(z^{\min})\right)^{-1} Y_{\rightarrow}^{(+)}(z^{\min}), \quad T_{\rightarrow} = \left(X^{(+)}(z^{\max})\right)^{-1} \Phi_{\rightarrow}^{h}(z^{\max}).$$

3.3 Algorithm for Calculating the Complex Eigenvalues and Eigenfunctions of Metastable States

To calculate a complex eigenvalue and the corresponding eigenfunction a discrete problem is solved for the equation

$$\mathcal{F}(u) = 0, \quad \Leftrightarrow \quad \left\{ \mathcal{F}_1(u) = 0, \quad \mathcal{F}_2(u) = 0 \right\} \tag{36}$$

with respect to the pair of unknowns $u = \{E^h, \mathbf{\Phi}^h\}$, where $\mathcal{F}_1(u)$ and $\mathcal{F}_2(u)$ are given by the expressions

$$\mathcal{F}_1(u) = \left[\mathbf{A} - 2E^h\mathbf{B} + \mathbf{M}_{\min}(E^h) - \mathbf{M}_{\max}(E^h)\right]\mathbf{\Phi}^h, \quad \mathcal{F}_2(u) = (\mathbf{\Phi}^h)^T\mathcal{F}_1(u).$$

The transition from the approximate solution u_k to the approximate solution u_{k+1} is given by the formulas

$$2E_{k+1}^h = 2E_k^h + \mu_k\tau_k, \quad \Phi_{k+1}^h = \mathbf{\Phi}_k^h + \mathbf{v}_k\tau_k, \tag{37}$$

$$\mathbf{v}_k = \mathbf{v}_k^{(1)} + \mathbf{v}_k^{(2)}\mu_k, \quad \mathbf{\Phi}_{k+1}^h = \mathbf{\Phi}_{k+1}^h((\mathbf{\Phi}_{k+1}^h)^T\mathbf{B}\mathbf{\Phi}_{k+1}^h)^{-1/2},$$

where $2E^h_{k=0} = 2E_0$, $\mathbf{\Phi}^h_{k=0} = \mathbf{\Phi}_0$ is the initial approximation from the vicinity of the solution $2E = 2E_*$, $\mathbf{\Phi}^h = \mathbf{\Phi}_*$. The iteration corrections $\mathbf{v}^{(1)}_k$, $\mathbf{v}^{(2)}_k$ are found by solving the inhomogeneous algebraic problems

$$\mathcal{F}_1(E^h_k, \mathbf{v}^{(1)}_k) = -\mathcal{F}_1(E^h_k, \mathbf{\Phi}^h_k) = -\mathcal{F}_1(u_k), \quad \Rightarrow \quad \mathbf{v}^{(1)}_k = -\mathbf{\Phi}^h_k, \tag{38}$$

$$\mathcal{F}_1(E^h_k, \mathbf{v}^{(2)}_k) = \left(\mathbf{B} - \frac{d\mathbf{M}_{\min}(E^h_k)}{2dE^h_k} + \frac{d\mathbf{M}_{\max}(E^h_k)}{2dE^h_k}\right)\mathbf{\Phi}^h_k, \tag{39}$$

and the correction μ_k to the eigenvalue E^h_k is found using the formula

$$\mu_k = \frac{\mathcal{F}_2(E^h_k, \mathbf{\Phi}^h_k)}{(\mathbf{\Phi}^h_k)^T\mathbf{B}\mathbf{\Phi}^h_k} \equiv \frac{(\mathbf{\Phi}^h_k)^T\mathcal{F}_1(E^h_k, \mathbf{\Phi}^h_k)}{(\mathbf{\Phi}^h_k)^T\mathbf{B}\mathbf{\Phi}^h_k},$$

that follows from Eq. (36). The expressions for nonzero elements of $\mathbf{M}_{\min}(E^h_k)$, $\mathbf{M}_{\max}(E^h_k)$, and their derivatives by $2E^h_k$ have the form ($L' = L + 1 - \kappa^{\max}$)

$$(\mathbf{M}_{\min}(E^h_k))_{11} = -f_2(z^{\min})\sqrt{-2E^h_k}, \quad (\mathbf{M}_{\max}(E^h_k))_{L',L'} = f_2(z^{\max})\sqrt{-2E^h_k},$$

$$\frac{d(\mathbf{M}_{\min}(E^h_k))_{11}}{d(2E^h_k)} = \frac{f_2(z^{\min})}{2\sqrt{-2E^h_k}}, \quad \frac{d(\mathbf{M}_{\max}(E^h_k))_{L',L'}}{d(2E^h_k)} = -\frac{f_2(z^{\max})}{2\sqrt{-2E^h_k}}.$$

The iteration step τ_k in the vicinity of the solution is equal to one, and the optimal step τ_k is calculated using the formula [24]

$$\tau_k = \max\left(\theta, \delta_k(0)/(\delta_k(0) + \delta_k(1))\right), \quad \theta = 0.1.$$

Here $\delta_k(0) = |\mathcal{F}_1(E^h_k, \mathbf{\Phi}^h_k)|^2$ and $\delta_k(1) = |\mathcal{F}_1(E^h_{k+1}, \mathbf{\Phi}^h_{k+1})|^2$ are the residuals and E_{k+1} and $\mathbf{\Phi}^h_{k+1}$ are calculated using Eqs. (37) at $\tau_k = 1$. In all cases $\theta < \tau_k < 1$. The iteration process (37) is terminated, when the condition $|\mathcal{F}_2(E^h_k, \mathbf{\Phi}^h_k)|^2 < \varepsilon$ becomes valid, where $\varepsilon > 0$ is the predetermined accuracy of the approximate solution calculation.

4 Benchmark Calculations

As an example, let us consider the Schrödinger equation (1) at $f_1(z) = f_2(z) = 1$ with the complex Scarf potential on the axis $z \in (-\infty, +\infty)$:

$$V_{Scarf}(z) = V_1 \cosh^{-2} z + \imath V_2 \sinh z \cosh^{-2} z. \tag{40}$$

Problem 1. For $V_1 < 0$ and $V_2^2 \in \mathcal{R}$ the bound state problem has a finite set of known analytic solutions [12]. At $|V_2| < 1/4 - V_1$ the eigenvalues are essentially complex conjugate pairs:

$$E^{\pm}_n = -\left(n - (g^*_+ \pm \imath g^*_- - 1)/2\right)^2,\ g^*_{\pm} = \sqrt{1/4 - V_1 \mp V_2},\ n = 0, 1, \ldots < (g^*_+ - 1)/2. \tag{41}$$

At $|V_2| > 1/4 - V_1$ (or when V_2 is imaginary) the eigenvalues are real:

$$E_n = -\left(n - (g^*_+ + g^*_- - 1)/2\right)^2, \quad n = 0, 1, \ldots < (g^*_+ + g^*_- - 1)/2. \tag{42}$$

Table 1. Eigenvalues $E_1^{\pm}$, E_1 and their differences from the corresponding analytic values calculated using the grid $(-20(N_1) - 4(N_2)4(N_3)20)$ with the number $N_1{=}N_2{=}N_3$ of the eighth-order finite elements ($\kappa_{\max}{=}3$, $p{=}2$) in each of the subintervals, depending on N_1. The last row presents the analytic values and the Runge coefficient (43).

N_1	$V_1 = -2$, $V_2 = -3$		$V_1 = -2$, $V_2 = -1$	
4	−0.229080666±0.559461207*I	2.8E– 4∓3.1E–4*I	−0.921836165	5.4E–4+6E–14*I
8	−0.229357025±0.559142713*I	–9.5E– 7±1.3E–6*I	−0.922378370	–9.6E–7–6E–13*I
16	−0.229356076±0.559144037*I	3E–10±2.5E–9*I	−0.922377406	–6 E–10–3E–11*I
ext	−0.229356076±0.559144040*I	$Ru = 8.005$	−0.922377405	$Ru = 9.130$

Table 2. Dependence of the coefficients of transmission T, reflection R, and absorption A, calculated using the grid $(-20(N_1)20)$ upon the number N_1 of the eighth-order finite elements ($\kappa_{\max} = 3$, $p = 2$) for $V_1 = 2$, $V_2 = 2$, $k = 2E = 1$. The last two rows present the analytical solution and the Runge coefficient (43).

N_1	Digits	$T_{\rightarrow}$	$R_{\rightarrow}$	$A_{\rightarrow}$
20	16	0.6005954018870188	0.0007394643169153872	0.3986651337960658
40	16	0.5984475588608321	0.0007498888028424546	0.4008025523363254
80	16	0.5984514912751766	0.0007498689244704378	0.4007986398003530
80	8	0.59845983	0.00074979961	0.4007903704
ext		0.5984515130037975	0.0007498688034693990	0.4007986181927332
Ru	16	9.088	9.029	9.088

The numerical experiments using the finite-element grid $\Omega^p_{h_j(z)}[z^{\min}, z^{\max}]$ demonstrated strict correspondence to the theoretical estimations (20) for both eigenvalues and eigenfunctions. In particular, we calculated the Runge coefficients

$$\beta_l = \log_2 \left| (\sigma_l^h - \sigma_l^{h/2})/(\sigma_l^{h/2} - \sigma_l^{h/4}) \right|, \quad l = 1, 2, \tag{43}$$

on three twice condensed grids with the absolute errors

$$\sigma_1^h = |F(E_m^{exact}) - F(E_m^h)|, \quad \sigma_2^h = \max_{z \in \Omega^h(z)} |\Phi_m^{exact}(z) - \Phi_m^h(z)| \tag{44}$$

for the eigenvalues and eigenfunctions, respectively. From Eq. (44) we obtained the numerical assessment of the convergence order $Ru \sim 8 \div 9$ of the proposed numerical schemes (shown for $F(E) = E$ in Table 1 and for $F(E) = T_{\rightarrow}, R_{\rightarrow}, A_{\rightarrow}$ in Table 2), the theoretical estimates being $\beta_1 = p' + 1$ and $\beta_2 = p' + 1$, in accordance with the *Remark* following Eq. (20).

Problem 2. For the scattering problem with fixed real-valued energy $2E = k^2 > 0$ and the complex Scarf potential (40) the coefficients of transmission $|T|^2$ and reflection $|R|^2$ are expressed as

$$|R_{\rightarrow}|^2=D_{\rightarrow}/D, \quad |R_{\leftarrow}|^2=D_{\leftarrow}/D, \quad |T_{\rightarrow}|^2=|T_{\leftarrow}|^2=\sinh^2(2\pi k)/D, \tag{45}$$
$$D_{\rightarrow} = (2\cosh(\pi g_+)\cosh(\pi g_-)+\cosh^2(\pi g_+)e^{-2\pi k}+\cosh^2(\pi g_-)e^{2\pi k}),$$
$$D_{\leftarrow} = (2\cosh(\pi g_+)\cosh(\pi g_-)+\cosh^2(\pi g_+)e^{2\pi k}+\cosh^2(\pi g_-)e^{-2\pi k}),$$
$$D=\sinh^2(2\pi k)+2\cosh(2\pi k)\cosh(\pi g_+)\cosh(\pi g_-)+\cosh^2(\pi g_+)+\cosh^2(\pi g_-).$$

Here the notation $g_{\pm}=\sqrt{V_1 \pm V_2-1/4}$ is used. It has been proved [11] that when the potential is complex and spatially non-symmetric, the reflectivity depends on whether the particle is incident from the left or the right side. For the complex potential scattering with the fixed real $E > 0$ the conditions (15) are modified as follows:

$$|R_{\rightarrow}|^2 + |T_{\rightarrow}|^2 = 1 - A_{\rightarrow}, \quad |R_{\leftarrow}|^2 + |T_{\leftarrow}|^2 = 1 - A_{\leftarrow}, \quad T_{\rightarrow} = T_{\leftarrow} \equiv T.$$

For the complex Scarf potential $A_{\rightarrow}$ and $A_{\leftarrow}$ are expressed as

$$A_{\rightarrow}=\frac{s_+s_- - s_-^2}{1+s_+s_-}, \quad A_{\leftarrow}=\frac{s_+s_- - s_+^2}{1+s_+s_-}, \quad s_{\pm}=\frac{\cosh(\pi g_+)e^{\pm\pi k}+\cosh(\pi g_-)e^{\mp\pi k}}{\sinh(2\pi k)}. \tag{46}$$

Here we consider only positive values $A_{\rightarrow} > 0$ (or $A_{\leftarrow} > 0$), commonly interpreted as the probability of absorption [11, 13].

The *Problem 1* of determining the eigenvalues E_m^h and the corresponding eigenfunctions $\Phi_m^h(z)$ for Eq. (19) was solved using the built-in package LinearAlgebra of the Maple system. Table 1 presents the dependence of the eigenvalues calculated using the grid $(-20(N_1) - 4(N_2)4(N_3)20)$ with the number $N_1 = N_2 = N_3$ of the eighth-order finite elements ($\kappa_{\max} = 3$, $p = 2$) in each of the subintervals upon N_1. One can see that these sequences converge to the analytical results (41) and (42). The behaviour of the eigenfunctions $\Phi_m^h(z)$ is illustrated by Fig. 1. The time of computing the auxiliary integrals is nearly 42 seconds, the time of constructing the matrices and solving the algebraic eigenvalue problem at $N = 16$ amounts to 4.5 seconds. Table 2 illustrates the dependence of the coefficients of transmission T, reflection R, and absorption A calculated using the grid $(-20(N_1)20)$ upon the number N_1 of the eighth-order finite elements ($\kappa_{\max} = 3$, $p = 2$). One can see that these sequences converge to the analytical results (45) and (46) . The time of constructing the matrices and solving the algebraic problem for $N_1 = 20$ and $N_1 = 80$ (Digits:=16) amounts to 5 and 22 seconds, respectively, and for $N_1 = 80$ (Digits:=8) this time is 5 seconds.

For a system of multiple-barrier Scarf potentials separated from each other the approximate analytic expressions for the coefficients of transmission, reflection, and absorption are also available. In particular, for a system of two Scarf potential the analytic expressions are presented in Ref. [13]).

The scattering *Problem 2* with Eqs. (21) and (30) was solved following the algorithm of Sections 3.1 and 3.2 and using the built-in package LinearAlgebra of the Maple system using the finite-element grid $(-8(N_1 = 40)8)$ c N_1 with Hermite eighth-order finite elements ($\kappa_{\max} = 3$, $p = 2$). The dependence upon k for the coefficients of transmission, reflection, and absorption, calculated with

Table 3. The first resonance energy values $2E_i^{\max T}$ for the maximal transmission coefficient (full transparency) and the eigenvalues $2E_i^r$ of resonance metastable states.

Scarf	$V_1 = 2$	$2E_1^{\max T} = 0.310918$	$2E_1^r = 0.31093782 - \imath 0.00069129$
	$V_2 = 0$	$2E_2^{\max T} = 1.025359$	$2E_2^r = 1.02413913 - \imath 0.01733149$
	$V_1 = 2$	$2E_1^{\max T} = 0.360240$	$2E_1^r = 0.36025570 - \imath 0.00103794$
	$V_2 = 1$	$2E_2^{\max T} = 1.036324$	$2E_2^r = 1.03383748 - \imath 0.02383030$
Steps/	$V_1 = 2$	$2E_1^{\max T} = 0.329476$	$2E_1^r = 0.32921557 - \imath 0.00247662$
wells	$V_2 = 0$	$2E_2^{\max T} = 1.254400$	$2E_2^r = 1.25175270 - \imath 0.03351010$
	$V_1 = 2$	$2E_1^{\max T} = 0.331776$	$2E_1^r = 0.33292316 - \imath 0.00247662$
	$V_2 = 1/2$	$2E_2^{\max T} = 1.263376$	$2E_2^r = 1.26054650 - \imath 0.03359483$

the absolute accuracy 0.001, in the system of two Scarf potentials with $V_1 = 2$, $V_2 = 1$ separated by the interval $d = 7/2$, is presented in the upper panel of Fig. 2. The resonance structure of the transmission coefficient is due to the presence of metastable states submerged in the continuous spectrum.

Problem 3. The complex eigenvalues and the corresponding eigenfunctions of the metastable states are calculated by means of the Newton iteration algorithm of Section 3.3 using the built-in package LinearAlgebra of the Maple system. For the initial approximation we used both the solutions of the bound-state *Problem 1* and the solutions of the scattering *Problem 2* with the resonance values of energy $E = E^r$, corresponding to the peaks of the transmission coefficient.

For the system of two real- and complex-valued Scarf potentials Fig. 3 presents the wave functions of the scattering problem for the first resonance state, corresponding to the maximal transmission coefficient (full transparency), and the functions of a resonance metastable state. The first resonance energy values $2E_i^{\max T}$ corresponding to the maximal transmission coefficient (full transparency) and the eigenvalues $2E_i^r$ of the resonance metastable states are shown in Table 3. The calculations were performed using the grid $(-8(N_1 = 40)8)$ with N_1 Hermite eighth-order finite elements ($\kappa_{\max} = 3$, $p = 2$).

In a similar way the piecewise continuous potentials are considered, in particular, the systems of potential steps/wells with rectangular-shaped walls. The latter problem can be solved analytically. The lower panel of Fig. 2 presents the approximation of the system of two Scarf potentials with a system of potential steps/wells. As seen from Fig. 2, with the increase of the wave number k the transmission, reflection, and absorption coefficients differ stronger. The calculations were performed using the grid $(-7(N_1{=}10){-}2{-}7/4(N_2{=}3){-}2{-}7/8(N_3{=}3)$ $-2(N_4{=}20)2(N_5{=}3)2{+}7/8(N_6{=}3)2{+}7/4(N_7{=}10)7)$ with N_i $(i = 1, ..., 7)$ Hermite seventh-order finite elements ($\kappa_{\max}{=}2$, $p = 3$). The eigenvalues for the system of real and complex potential steps/wells (see Table 3) qualitatively agree with the results presented in the above paragraph. The scattering wave functions for the first two resonance energy values and for the resonance metastable states behave qualitatively similar to those of the system of Scarf potentials, and for this reason are not presented here.

5 Conclusion

The presented analysis of solving the eigenvalue problem, the scattering problem, and the calculation of resonance metastable states for the Schrödinger equation with continuous and piecewise continuous real-valued and complex potentials demonstrated the efficiency of the developed algorithms and programs, implemented in the Maple computer algebra system. The algorithm conserves the derivative continuity property, inherent in the desired solution, in the approximating numeric solution, defined on the finite-element grid using the Hermite interpolating elements.

Further development of the proposed algorithms and programs is targeted at the solution of the problems that describe the scattering processes in the quantum-dimensional semiconductor systems and smoothly irregular waveguides with piecewise continuous real-valued and complex coefficient functions in the partial differential equations, which require the continuity of not only the solution itself, but also of its first derivative.

The authors thank Prof. V.P. Gerdt for collaboration and support of this work. The work was partially supported by the Russian Foundation for Basic Research (RFBR) (grants No. 14-01-00420 and 13-01-00668), the Bogoliubov-Infeld and the Hulubei-Meshcheryakov JINR-Romania programs.

References

1. Kotlyar, V.V., Kovalev, A.A., Nalimov, A.G.: Gradient microoptical elements for achieving superresolution. Kompyuternaya optika **33**, 369–378 (2009). (in Russian)
2. Rezanur Rakhman, K.M., Sevastyanov, L.A.: One-dimensional scattering problem at stepwise potential with non-coincident asymptotic forms. Vestnik RUDN, ser. Fizika No. 5 (1), 35–38 (1997) (in Russian)
3. Sevastyanov, L.A., Sevastyanov, A.L., Tyutyunnik, A.A.: Analytical calculations in maple to implement the method of adiabatic modes for modelling smoothly irregular integrated optical waveguide structures. In: Gerdt, V.P., Koepf, W., Seiler, W.M., Vorozhtsov, E.V. (eds.) CASC 2014. LNCS, vol. 8660, pp. 419–431. Springer, Heidelberg (2014)
4. Chuluunbaatar, O., Gusev, A.A., Gerdt, V.P., Kaschiev, M.S., Rostovtsev, V.A., Samoylov, V., Tupikova, T., Vinitsky, S.I.: A symbolic-numerical algorithm for solving the eigenvalue problem for a hydrogen atom in the magnetic field: cylindrical coordinates. In: Ganzha, V.G., Mayr, E.W., Vorozhtsov, E.V. (eds.) CASC 2007. LNCS, vol. 4770, pp. 118–133. Springer, Heidelberg (2007)
5. Gusev, A.A., Chuluunbaatar, O., Gerdt, V.P., Rostovtsev, V.A., Vinitsky, S.I., Derbov, V.L., Serov, V.V.: Symbolic-numeric algorithms for computer analysis of spheroidal quantum dot models. In: Gerdt, V.P., Koepf, W., Mayr, E.W., Vorozhtsov, E.V. (eds.) CASC 2010. LNCS, vol. 6244, pp. 106–122. Springer, Heidelberg (2010)
6. Gusev, A.A., Vinitsky, S.I., Chuluunbaatar, O., Gerdt, V.P., Rostovtsev, V.A.: Symbolic-numerical algorithms to solve the quantum tunneling problem for a coupled pair of ions. In: Gerdt, V.P., Koepf, W., Mayr, E.W., Vorozhtsov, E.V. (eds.) CASC 2011. LNCS, vol. 6885, pp. 175–191. Springer, Heidelberg (2011)

7. Vinitsky, S., Gusev, A., Chuluunbaatar, O., Rostovtsev, V., Le Hai, L., Derbov, V., Krassovitskiy, P.: Symbolic-numerical algorithm for generating cluster eigenfunctions: tunneling of clusters through repulsive barriers. In: Gerdt, V.P., Koepf, W., Mayr, E.W., Vorozhtsov, E.V. (eds.) CASC 2013. LNCS, vol. 8136, pp. 427–442. Springer, Heidelberg (2013)
8. Vinitsky, S., Gusev, A., Chuluunbaatar, O., Le Hai, L., Góźdź, A., Derbov, V., Krassovitskiy, P.: Symbolic-numeric algorithm for solving the problem of quantum tunneling of a diatomic molecule through repulsive barriers. In: Gerdt, V.P., Koepf, W., Seiler, W.M., Vorozhtsov, E.V. (eds.) CASC 2014. LNCS, vol. 8660, pp. 472–490. Springer, Heidelberg (2014)
9. Gusev, A.A., Chuluunbaatar, O., Vinitsky, S.I., Abrashkevich, A.G.: KANTBP 3.0: New version of a program for computing energy levels, reflection and transmission matrices, and corresponding wave functions in the coupled-channel adiabatic approach. Comput. Phys. Commun. **185**, 3341–3343 (2014)
10. Molinàs-Mata, P., Molinàs-Mata, P.: Electron absorption by complex potentials: One-dimensional case. One-dimensional case. Phys. Rev. A **54**, 2060–2065 (1996)
11. Ahmed, Z.: Schrödinger transmission through one-dimensional complex potentials. Phys. Rev. A **64**, 042716 (2001)
12. Ahmed, Z.: Real and complex discrete eigenvalues in an exactly solvable one-dimensional complex PT -invariant potential. Phys. Lett. A **282**, 343–348 (2001)
13. Cerveró, J.M., Rodríguez, A.: Absorption in atomic wires. Phys. Rev. A **70**, 052705 (2004)
14. Muga, J.G., Palao, J.P., Navarro, B., Egusquiza, I.L.: Complex absorbing potentials. Phys. Reports **395**, 357–426 (2004)
15. Cannata, F., Dedonder, J.-P., Ventura, A.: Scattering in PT-symmetric quantum mechanics. Annals of Physics **322**, 397–433 (2007)
16. Becker, E.B., Carey, G.F., Oden, T.J.: Finite elements. An introduction, vol. I. Prentice-Hall Inc., Englewood Cliffs (1981)
17. Ram-Mohan, R.L.: Finite Element and Boundary Element Aplications in Quantum Mechanics. Oxford University Press, New York (2002)
18. Amodio, P., Blinkov, Y., Gerdt, V., La Scala, R.: On consistency of finite difference approximations to the navier-stokes equations. In: Gerdt, V.P., Koepf, W., Mayr, E.W., Vorozhtsov, E.V. (eds.) CASC 2013. LNCS, vol. 8136, pp. 46–60. Springer, Heidelberg (2013)
19. Gusev, A.A., Chuluunbaatar, O., Vinitsky, S.I., Derbov, V.L., Góźdź, A., Le Hai, L., Rostovtsev, V.A.: Symbolic-numerical solution of boundary-value problems with self-adjoint second-order differential equation using the finite element method with interpolation hermite polynomials. In: Gerdt, V.P., Koepf, W., Seiler, W.M., Vorozhtsov, E.V. (eds.) CASC 2014. LNCS, vol. 8660, pp. 138–154. Springer, Heidelberg (2014)
20. Berezin, I.S., Zhidkov, N.P.: Computing Methods, vol. I. Pergamon Press, Oxford (1965)
21. Strang, G., Fix, G.J.: An Analysis of the Finite Element Method. Prentice-Hall, Englewood Cliffs (1973)
22. Kukulin, V.I., Krasnopol'sky, V.M., Horáček, J.: Theory of Resonances, pp. 107–112. Academia, Praha (1989)
23. Siegert, A.J.F.: On the derivation of the dispersion formula for nuclear reactions. Phys. Rev. **56**, 750–752 (1939)
24. Ermakov, V.V., Kalitkin, N.N.: The optimal step and regularization for Newton's method. USSR Computational Mathematics and Mathematical Physics **21**, 235–242 (1981)